Paper IX

Sølve Selstø, Alicia Palacios, Jorge Fernández, and Fernando Martín

Electron angular distribution in resonance enhanced two-photon ionization of H_2^+ by ultrashort laser pulses

To be submitted to Physical Review.

Electron angular distribution in resonance enhanced two-photon ionization of H_2^+ by ultrashort laser pulses

S. Selstø*, A. Palacios, J. Fernández, and F. Martín
Departamento de Química C-9, Universidad Autónoma de Madrid, 28049 Madrid, Spain.
(Dated: June 22, 2006)

We present a theoretical study of the electron angular distribution produced in resonance enhanced two-photon ionization of the H_2^+ molecular ion using ultrashort laser pulses. The method consists in solving the time dependent Schrödinger equation and includes all electronic and vibrational degrees of freedom. Differential (in proton energy and electron emission solid angle) ionization probabilities have been evaluated for various photon energies, laser intensities and pulse durations. We show that (1+1)-REMPI leads to angular distributions significantly different from those produced in direct two-photon ionization. The REMPI process is observed even at photon energies not matching the energy difference between two electronic states in a perfect vertical transition. Interestingly, there is no trace of REMPI effects when the fully differential probabilities are integrated over proton energy.

PACS numbers: 33.80.Rv, 33.80.-b,

I. INTRODUCTION

Experimental approaches that make use of high-order harmonic generation [1, 2] or free electron lasers [3–5] are currently able to provide fs laser pulses with wave lengths in the VUV/XUV region of the electromagnetic spectrum. The use of such pulses has opened up the way to study elementary two- and three-photon ionization processes in simple atoms (He, Ne, ...) [6, 7] and molecules (H_2^+, H_2, ...) [8]. These systems are accessible to accurate theoretical descriptions, which is crucial to guide theoretical developments in strong field multiphoton ionization and to reach a deeper insight on the basic mechanisms involved in the latter process.

The study of multiphoton ionization in molecules is interesting because vibration and rotation may significantly affect the ionization process. This is the case of, e.g., resonance enhanced multiphoton ionization (REMPI), in which the molecule may have enough time to vibrate in the intermediate electronic state before it absorbs the additional photons that ultimately lead to ionization [9, 10]. Theoretical investigations of multiphoton ionization in molecules are scarce due to the difficulty to account for both electronic and nuclear degrees of freedom. Detailed investigations on H_2^+ ionization have been carried out in the infra-red (IR) regime (see [11] and references therein), mainly using low dimensional approaches. In the XUV domain, multiphoton ionization of H_2^+ has been recently studied by solving the time dependent Schrödinger equation (TDSE) within the frozen nuclei approximation (FNA) [12–15] or by including the effect of nuclear vibrations through perturbative [16] as well as non-perturbative [17, 18] approaches. The importance of the nuclear motion in the study of REMPI effects in H_2^+ by using XUV/fs pulses has been recently investigated by Palacios et al [9, 19] (these authors have recently extended these studies to the H_2 molecule [10]). The results of the latter investigations have shown that, at variance with atoms, electronic resonance effects do not lead to narrow peaks in the photoelectron energy spectra. This is because the electronic resonances are diluted among the different dissociative states. In contrast, resonance effects are perfectly visible when one analyzes the kinetic energy distribution (KED) of the nuclear fragments. None of these full dimensional theoretical studies have analyzed the electron angular distribution arising with such XUV pulses.

The aim of the present work is to theoretically investigate the electron angular distributions arising in two-photon ionization of H_2^+ by XUV/fs laser pulses including all electronic and vibrational degrees of freedom. We will pay special attention to the (1+1) REMPI region. Production of H_2^+ molecules in a well defined vibrational state (e.g. $v = 0$) is now possible and has in fact recently been used to study non ionizing dissociation dynamics [20] and tunnelling ionization [21]. Therefore, the present theoretical predictions should be amenable for comparison with experiment in the near future.

The paper is organized as follows. In section II we describe the theoretical methods used in the present work, in particular how the effect of the nuclear motion is introduced in our solution of the time dependent Schrödinger equation and how the electron angular distributions is extracted from this solution. The results for the angular distribution of photoelectrons, both differential in and integrated over the proton kinetic energy, are presented and discussed in section III. Conclusions are drawn in section IV. Atomic units are used throughout unless otherwise stated.

II. THEORY

We restrict our study to two-photon ionization of H_2^+ from the $X^2\Sigma_g^+(1s\sigma_g)$ ground state using linearly polar-

*Present address: Department of Physics and Technology, University of Bergen, N-5007 Bergen, Norway

ized light within the dipole approximation. We only consider the case of H_2^+ molecules oriented along the polarization direction of the incident light. In this particular case, the dipole selection rule implies that $\Delta m = 0$ and, therefore, that the first photon couples the initial molecular state to intermediate states of σ_u symmetry and the second photon couples the latter to final states of σ_g symmetry according to the sequence: $\sigma_g \rightarrow \sigma_u \rightarrow \sigma_g$. We solve the time-dependent Schrödinger equation (TDSE)

$$i\frac{\partial}{\partial t}\Phi(\mathbf{r}, R, t) = [H + V(t)]\Phi(\mathbf{r}, R, t) \tag{1}$$

where H is the Hamiltonian of H_2^+ in the body-fixed frame and $V(t) = \mathbf{p} \cdot \mathbf{A}(t)$ is the laser-molecule interaction potential in the velocity gauge. The vector $\mathbf{r}$ indicates all electronic coordinates and R is the internuclear distance. For a photon energy ω and a pulse duration T, the vector potential $\mathbf{A}(t)$, polarized along the vector $\mathbf{e}_z$ (the direction of the internuclear axis), is defined as

$$\mathbf{A}(t) = \begin{cases} A_0 \cos^2\left(\frac{\pi}{T}t\right)\cos(\omega t)\mathbf{e}_z\,; & t \in [-T/2, +T/2] \\ 0\,; & \text{elsewhere}\,. \end{cases} \tag{2}$$

The time-dependent molecular wave function $\Phi(\mathbf{r}, R, t)$ is expanded in the basis of stationary states $\Psi_{nv_n}(\mathbf{r}, R)$:

$$\Phi(\mathbf{r}, R, t) = \sum_n \sum\!\!\!\!\!\!\int_{v_n} c_{nv_n}(t)\Psi_{nv_n}(\mathbf{r}, R)\exp[-iW_{nv_n}t] + \sum_l \int d\varepsilon \sum\!\!\!\!\!\!\int_{v_\varepsilon} c^l_{\varepsilon v_\varepsilon}(t)\Psi^l_{\varepsilon v_\varepsilon}(\mathbf{r}, R)\exp[-iW_{\varepsilon v_\varepsilon}t] \tag{3}$$

where the first term is a summation over bound electronic states (and their corresponding vibrational states, including the dissociation continuum) and the second one is an integral over electronic continuum states for all l (including again the corresponding vibrational states). Substituting this expansion in the TDSE and neglecting non adiabatic couplings leads to a system of coupled differential equations that must be integrated over the whole pulse duration T to obtain the unknown coefficients c_{nv_n} and $c^l_{\varepsilon v_\varepsilon}$.

The methods we have used to solve the TDSE and obtain the stationary states used in the above expansion of the time dependent wave function are the same as those described in detail in Ref. [19]. Here we only summarize the main ingredients, paying special attention to the extraction of angular differential ionization probabilities. Neglecting rotational effects, the stationary states are written in the Born-Oppenheimer (BO) approximation:

$$\Psi_{nv_n}(\mathbf{r}, R) = R^{-1}\chi_{v_n}(R)\psi_n(\mathbf{r}, R) \tag{4}$$

where ψ_n and χ_{v_n} are the usual electronic and nuclear BO wave functions. For a given value of R, the electronic continuum states of energy $\varepsilon_n(R)$ satisfy the usual boundary conditions corresponding to a single incoming (outgoing) spherical wave with a well defined value of the angular momentum l and a combination of outgoing (incoming) spherical waves for all possible values of the angular momentum that are compatible with the molecular symmetry (see [22] for details).

In the ionization channel, the density of probability differential in both the proton kinetic energy and the solid angle of the emitted electron is given by

$$\frac{d^2P}{dE_{\mathrm{H}^+}d\Omega} = \int d\varepsilon \left|\sum_l i^{-l}e^{-i\sigma_l}Y_{l0}(\hat{k}_e)c^l_{\varepsilon v_\varepsilon}(t = T/2)\right|^2 \tag{5}$$

where E_{H^+} is the center-of-mass energy of the outgoing protons, Ω is the solid angle of the ionized electron, $\hat{k}_e$ is the corresponding wave vector direction, and σ_l is the Coulomb phase shift

$$\sigma_l = \arg\Gamma\left(l + 1 + iZ/k_e\right). \tag{6}$$

with $Z = 2$. Integrating equation (5) over the solid angle gives the density of probability differential in the proton kinetic energy,

$$\frac{dP}{dE_{\mathrm{H}^+}} = \sum_l \int d\varepsilon |c^l_{\varepsilon v_\varepsilon}(t = T/2)|^2 \tag{7}$$

and integrating further over vibrational energy gives the total ionization probability P, which is related to the cross section $\sigma(\mathrm{cm^4s}) = (\omega/I)^2(C/T)P$, where I is the laser intensity in $\mathrm{Wcm^{-2}}$, T is the pulse duration in seconds, ω is the photon energy in joules and $C = \frac{128}{35}$ is a dimensionless coefficient. T/C is an effective pulse duration [23] that takes into account the time dependence of the intensity.

All wave functions have been evaluated using B-spline basis sets following the procedures described in [24]. Briefly, vibrational wave functions have been expanded in a basis of 300 B-splines of order $k = 8$, contained in a box of 14 a.u.. Bound electronic states have been represented through a one-center expansion that includes spherical harmonics from $l = 0$ to $l = 12$. The corresponding radial parts have been expanded in a basis of 140 B-splines of order $k = 8$ in a box of radial length of 60 a.u.. By changing the box size and/or the number of basis functions, we have checked that this basis set leads to practically converged energies in the Franck-Condon (FC) region. For the final continuum states, we have used the L^2 close-coupling method (see [22] and references therein) in which each channel is represented in the same B-spline basis as that used for bound states. The resulting continuum states have the correct asymptotic behavior and exactly include inter-channel coupling within the box [22].

III. RESULTS AND DISCUSSION

We have solved the TDSE for various photon energies, laser intensities and pulse durations. We will concentrate on (1+1) REMPI processes similar to that shown

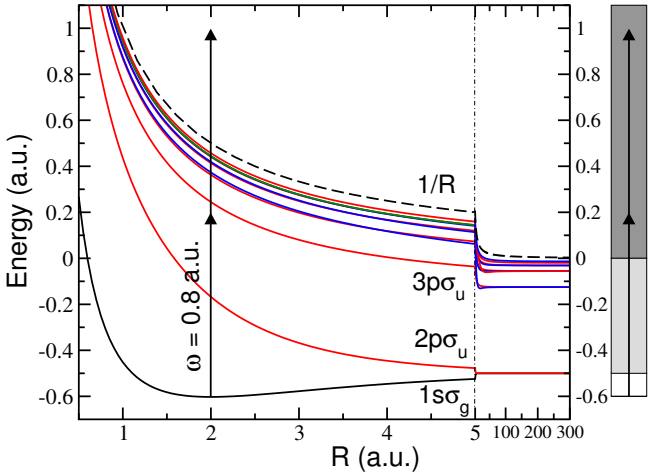

FIG. 1: *Color online*: Potential energy curves of H_2^+ as functions of internuclear distance. The figure shows the ground state, the ten lowest states of σ_u symmetry, and the ionization threshold $1/R$. A typical two-photon transition leading to (1+1)-REMPI is illustrated by arrows. The two shadowed areas in the right hand side column indicate dissociation and ionization+dissociation energy regions.

in Fig. 1 and, in particular, on the resonance features induced by the two lowest $^2\Sigma_u^+$ states of H_2^+. Figure 2 shows the electron angular distributions corresponding to different energies of the outgoing protons and three different photon energies, $\omega = 0.7$, 0.8 and 0.88 a.u.. In all cases, the laser intensity is 10^{12} Wcm^{-2} and the pulse duration 10 fs. To better understand the origin of the different structures observed in the angular distributions, the latter have been superimposed to the angle-integrated ionization probabilities differential in the proton kinetic energy. As explained in [9], the different peaks observed in the angle-integrated probability represent different physical processes: (*i*) direct non resonant two photon ionization (denoted by V), (*ii*) (1+1)-REMPI through the $^2\Sigma_u^+(2p\sigma_u)$ state (denoted by R_1), and (*iii*) (1+1)-REMPI through the $^2\Sigma_u^+(3p\sigma_u)$ state (denoted by R_2). It can be seen that, for proton energies lying in the non resonant region V, the photoelectron angular distribution follows the polarization direction and exhibits an almost pure *d* shape. This distribution is not very different to that observed in non resonant two-photon ionization of two-electron atomic systems like, e.g., H^- [25]. In contrast, for proton energies lying in the R_1 and R_2 resonance regions, the angular distribution is completely different: electrons are not only ejected along the polarization direction but also in a plane perpendicular to it. This behavior results from the important mixing between the $l = 0$ and $l = 2$ partial waves. Similar conclusions are obtained for the three photon energies considered in Fig. 2. It is important to stress here that the signature of the (1+1)-REMPI process is observed even though the photon energy does not match a vertical transition from the $X^2\Sigma_g^+$ ground state to any of the $^2\Sigma_u^+$ intermediate

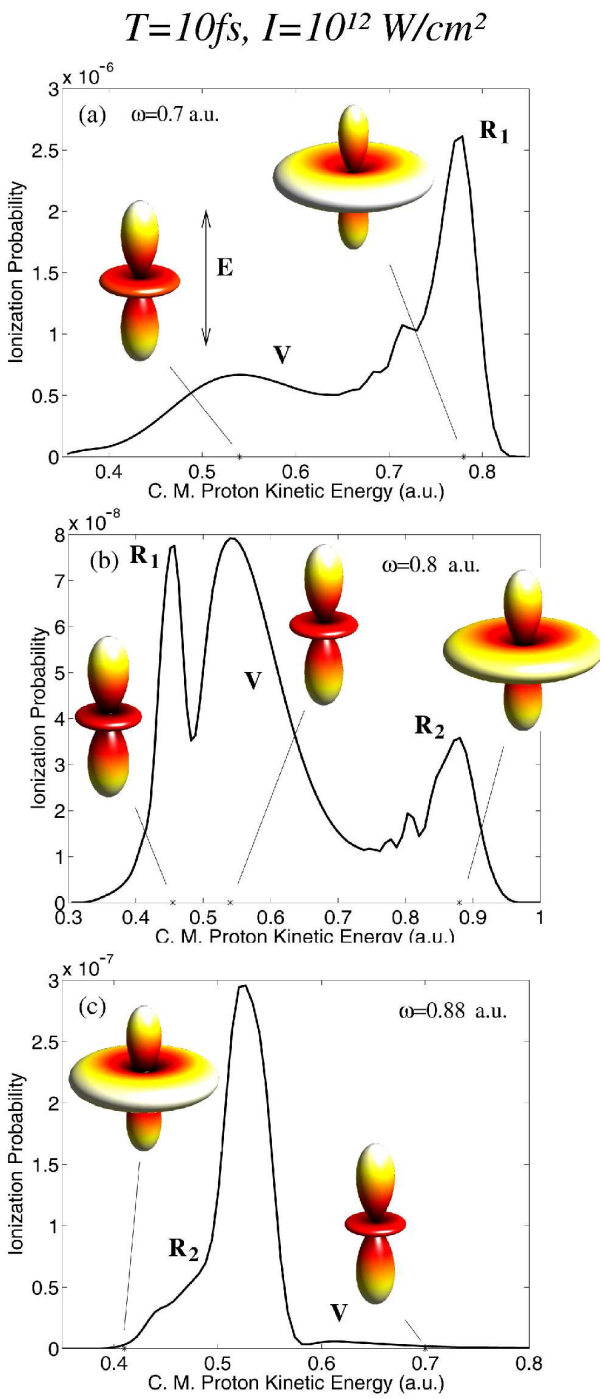

FIG. 2: *Color online*: Electron angular distributions corresponding to different energies of the outgoing protons for a laser intensity of 10^{12} Wcm^{-2} and pulse duration 10 fs. Three different photon energies have been considered: (a) $\omega = 0.7$, (b) 0.8 and (c) 0.88 a.u.. The angular distributions are superimposed to the angle-integrated ionization probabilities differential in the proton kinetic energy. C.M. means center of mass.

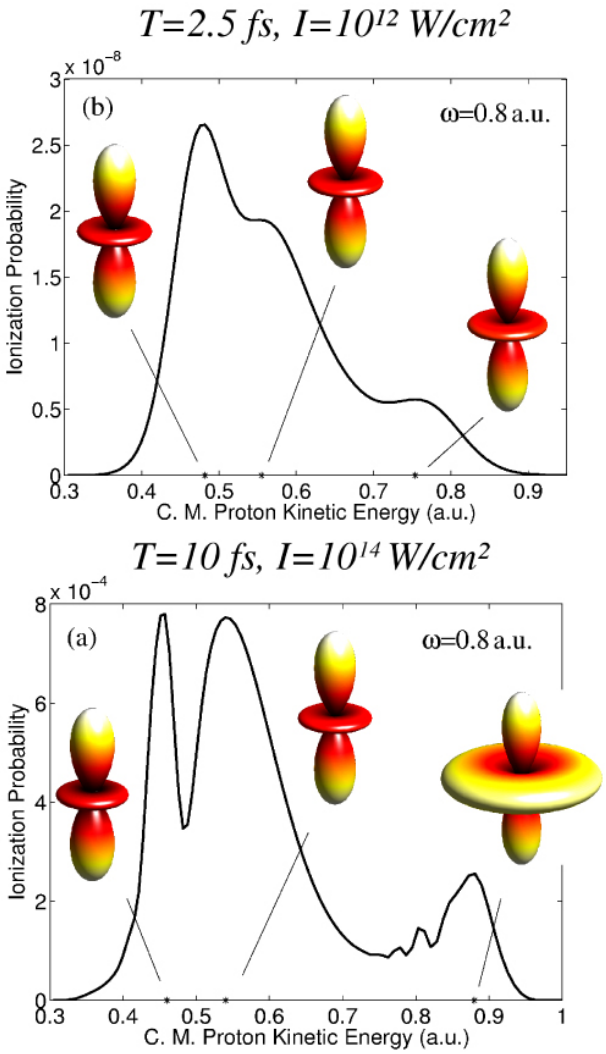

FIG. 3: *Color online*: Electron angular distributions corresponding to different energies of the outgoing protons for a laser intensity and pulse duration of (a) 10^{12} Wcm^{-2} and 2.5 fs, respectively, and (b) 10^{14} Wcm^{-2} and 10 fs. In both cases, the photon energy is $\omega = 0.8$ a.u.. The angular distributions are superimposed to the angle-integrated ionization probabilities differential in the proton kinetic energy. C.M. means center of mass.

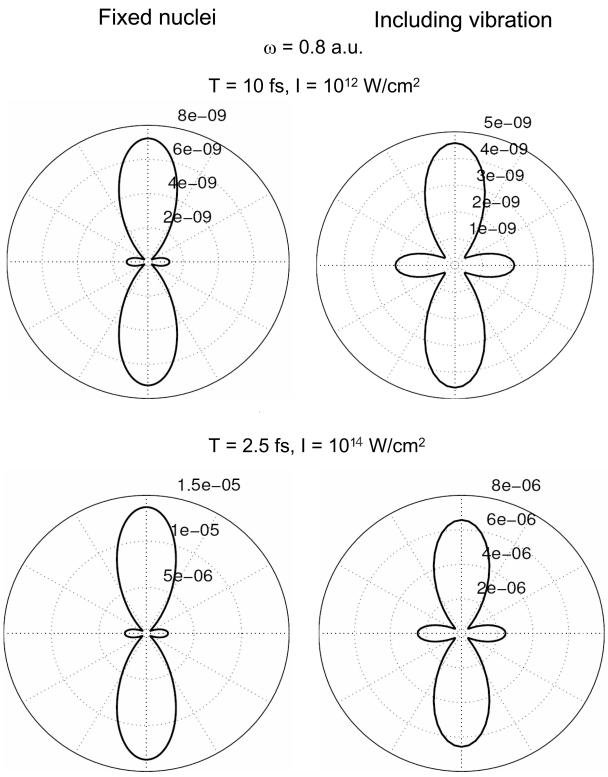

FIG. 4: Electron angular distributions integrated over proton kinetic energy. The photon energy is $\omega = 0.8$ a.u.. Top: $I = 10^{12}$ Wcm^{-2} and $T = 10$ fs. Bottom: $I = 10^{14}$ Wcm^{-2} and $T = 2.5$ fs. The left two panels show results obtained within the fixed-nuclei approximation.

states. The reason why the REMPI process is still visible under these circumstances is that the absorbed energy is shared by the electron and the nuclei. In practice, the energy sharing is only effective in the Franck-Condon region, but provided we are in that region, there is always a particular energy sharing for which a perfectly resonant electronic transition is possible at that photon energy.

For a pulse duration of 10 fs, the molecule has enough time to vibrate in the $^2\Sigma_u^+$ state resonantly populated by absorption of the first photon. This leads to the complex angular behavior shown in Fig. 2 near the R_1 and R_2 peaks. By reducing the pulse duration, there is less and less time to vibrate in the intermediate state and, therefore, one would expect, for all proton energies, an angular distribution similar to that of the non resonant process. This is illustrated in Fig. 3a where we show our results for a pulse of 2.5 fs and the same intensity. Not only are the R_1 and R_2 peaks diluted in the broad structure observed in the angle-integrated probability, but also the angular distribution is practically the same for all proton energies. A similar behavior is obtained when one increases the laser intensity keeping the pulse duration at 10 fs (see Fig. 3b). In this case, the higher intensity makes ionization more efficient and, therefore, there are less molecules that remain long enough in the intermediate state. As a consequence, the *d*-like distribution associated with the direct two-photon ionization process dominates.

It is also interesting to use the present results to check the validity of the fixed nuclei approximation (FNA), which is widely used to interpret ionization processes in molecular systems. In general, total ionization probabilities resulting from the FNA do not differ significantly from those obtained by including the nuclear motion, except in the resonance regions where the FNA leads to sharp peaks that are not physical [19]. Obviously, the FNA cannot be used to obtain probabilities that are dif-

ferential in the kinetic energy of the ionic fragments. But what about the electron angular distributions integrated over kinetic energy of these fragments? To answer this question, we show in Fig. 4 a comparison between the electron angular distributions obtained in the FNA and those resulting from the integration of the probabilities shown in Figs. 2 and 3 over proton energy. It can be seen that, apart from the absolute value of the calculated probabilities, the shapes of the angular distribution are very similar in both types of calculations and for both the longer and the shorter pulse. It is also apparent that, by integrating the angular distributions over proton energy, the signature of the REMPI effect disappears completely. We have checked that this is the case for all photon energies investigated in this work. Therefore, the only way to observe REMPI effects in the electron angular distribution is to analyze in addition the energy of the outgoing protons.

IV. CONCLUSION

We have theoretically studied the electron angular distribution that arises in resonance enhanced two-photon ionization of H_2^+ molecules oriented along the polarization vector by using ultrashort laser pulses in the XUV frequency domain. The theoretical method includes all electronic and vibrational degrees of freedom. We have found that the signature of the (1+1)-REMPI effect is to produce complex angular distributions that differ significantly from those observed in the direct two-photon ionization process (which have in term a marked atom-like character). The peculiar angular distributions associated with the REMPI process can only be observed by analyzing at the same time the proton kinetic energy distribution of the outgoing protons. Indeed, integration of the calculated fully differential probability over proton kinetic energy washes out the signature of the REMPI effect, thus suggesting that electron angular distributions obtained within the fixed-nuclei approximation are not appropriate to investigate this process. Interestingly, by analyzing the electron angular distributions as functions of proton energy, it is possible to observe REMPI even at photon energies that do not correspond necessarily to vertical transitions between two electronic states of the molecule. More theoretical work is needed to see if these predictions are of general validity.

Acknowledgments

Work supported by the DGI (Spain) project no. BFM2003-00194, the European COST action D26/0002/02, and the Norwegian Research Council. We thank the CCC-UAM (Madrid, Spain) for computer time.

[1] P. Agostini and L. F. DiMauro, Rep. Prog. Phys. **67**, 813 (2004).
[2] R. Klenberger, E. Goulielmakis, M. Uiberacker, A. Baltuska, V. Yakovlev, F. Bammer, A. Scrinzi, T. Westerwalbesloh, U. Kleineberg, U. Heinzmann, et al., Nature **427**, 817 (2004).
[3] J. Andruszkow et al., Phys. Rev. Lett. **85**, 3825 (2000).
[4] H. Wabnitz, L. Bittner, A. R. B. de Castro, R. Döhrmann, P. Gürtler, T. Laarmann, W. Laasch, J. Schulz, A. Swiderski, K. von Haeften, et al., Nature **420**, 482 (2002).
[5] V. Ayvazyan et al., Phys. Rev. Lett. **88**, 104802 (2002).
[6] N. Miyamoto, M. Kamei, D. Yoshitomi, T. Kanai, T. Sekikawa, T. Nakajima, and S. Watanabe, Phys. Rev. Lett. **93**, 083903 (2004).
[7] Y. Nabekawa, H. Hasegawa, E. J. Takahashi, and K. Midorikawa, Phys. Rev. Lett. **94**, 043001 (2005).
[8] K. Hoshina, A. Hishikawa, K. Kato, T. Sako, K. Yamanouchi, E. J. Takahashi, Y. Nabekawa, and K. Midorikawa, J. Phys. B **39**, 813 (2006).
[9] A. Palacios, H. Bachau, and F. Martín, J. Phys. B **38**, L99 (2005).
[10] A. Palacios, H. Bachau, and F. Martín, Phys. Rev. Lett. **96**, 173201 (2006).
[11] A. D. Bandrauk, S. Chelkowski, and I. Kawata, Phys. Rev. A **67**, 013407 (2003).
[12] D. Dundas, J. F. McCann, J. Parker, and K. T. Taylor, J. Phys. B **33**, 3261 (2000).
[13] J. Colgan, M. S. Pindzola, and F. Robicheaux, Phys. Rev. A **68**, 063413 (2003).
[14] S. Barmaki, S. Laulan, H. Bachau, and M. Ghalim, J. Phys. B **36**, 817 (2003).
[15] S. Selstø, M. Førre, J. P. Hansen, and L. B. Madsen, Phys. Rev. Lett. **95**, 093002 (2005).
[16] A. Apalategui, A. Saenz, and P. Lambropoulos, J. Phys. B **33**, 2791 (2000).
[17] S. Barmaki, H. Bachau, and M. Ghalim, Phys. Rev. A **69**, 043403 (2004).
[18] S. Selstø, J. F. McCann, M. Førre, J. P. Hansen, and L. B. Madsen, Phys. Rev. A **73**, 033407 (2006).
[19] A. Palacios, S. Barmaki, H. Bachau, and F. Martín, Phys. Rev. A **71**, 063405 (2005).
[20] K. Sändig, H. Figger, and T. W. Hänsch, Phys. Rev. Lett. **85**, 4876 (2000).
[21] B. Fabre, J. H. Posthumus, L. Malfaire, E. M. Staicu-Casagrande, J. Jureta, C. Cornaggia, E. Baldit, and X. Urbain, Laser Phys. **14**, 468 (2004).
[22] F. Martín, J. Phys. B **32**, R197 (1999).
[23] L. B. Madsen and P. Lambropoulos, Phys. Rev. A **59**, 4574 (1999).
[24] H. Bachau, E. Cormier, P. Decleva, J. E. Hansen, and F. Martín, Rep. Prog. Phys. **64**, 1815 (2001).
[25] I. Sánchez, H. Bachau, and F. Martín, J. Phys. B **30**, 2417 (1997).